NANO LETTERS

Letter

pubs.acs.org/NanoLett

Unique Determination of "Subatomic" Contrast by Imaging Covalent Backbonding

Adam Sweetman,*[,†] Philipp Rahe,[‡] and Philip Moriarty[†]

[†]The School of Physics and Astronomy, The University of Nottingham, Nottingham NG7 2RD, United Kingdom

[‡]Department of Physics and Astronomy, The University of Utah, Salt Lake City, Utah 84112, United States

Supporting Information

ABSTRACT: The origin of so-called "subatomic" resolution in dynamic force microscopy has remained controversial since its first observation in 2000. A number of detailed experimental and theoretical studies have identified different possible physicochemical mechanisms potentially giving rise to subatomic contrast. In this study, for the first time we are able to assign the origin of a specific instance of subatomic contrast as being due to the back bonding of a surface atom in the tip−sample junction.

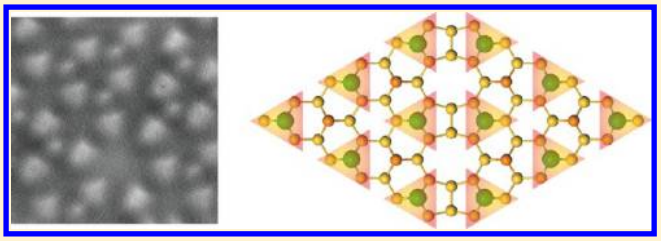

KEYWORDS: *NC-AFM, DFM, subatomic, Si(111), qPlus, UHV*

Since atomic resolution was first obtained by scanning probe microscopy (SPM),[1] scanning tunneling microscopy (STM) and atomic force microscopy (AFM) have become invaluable tools for both surface science and nanoscience. Despite more than 30 years of striking results, however, it is well-known that the interpretation of scanning probe images is often complicated due to the variety of tip structures that are observed. In recent years, a focus has developed on determining the structure of the very apex of the tip by combining experiment with detailed theoretical calculations[2−4] or by inverse imaging of the tip on a known surface moiety.[5−7] A parallel stream of work, pioneered by the group at IBM Zurich, involves the functionalization of a metal tip with a known molecule or atom in order to provide a well-defined termination. This has been key to both obtaining, and interpreting, striking submolecular resolution on planar organic molecules in dynamic force microscopy (DFM), also known as noncontact atomic force microscopy (NC-AFM).[8]

Although Giessibl et al. coined the term "subatomic contrast" in 2000[9] in relation to imaging of the Si(111)-(7 × 7) surface, their results were critiqued by Hug and co-workers.[10] In the work of Giessibl et al.,[9] features in the images of adatoms of the Si(111) surface were assigned to a "double lobe" tip and interpreted as resulting from an apex with a single terminating silicon atom having two exposed dangling bonds. Soon after publication, it was suggested that the features may have arisen as a result of feedback artifacts, in part based on the observation that the shape of the double lobes changed with reversal of the scan direction.[10] Subsequently, it was shown that these features could be reproduced with the lobes aligned in directions not perpendicular to the scan direction,[11] and theoretical calculations suggested that the double lobe features might indeed be observable.[12]

However, it should be noted that due to the computational constraints of the time these simulations involved a number of simplifications, including the use of very small tip-clusters and the fixing of the tips atoms during the calculation of the tip−sample forces. Later, more sophisticated calculations[13] performed without these limitations suggested that the original model put forward to explain the double lobe features was perhaps oversimplified, and, even if unphysically constrained, did not produce the "double lobe" features observed experimentally or observed in earlier simulations. In addition, other simulations[14] suggested that double lobe features might also arise from complex electron scattering effects, occurring during tunnelling into the surface adatoms at very specific biases from a double-lobe-terminated tip. The force calculations in this instance, however, assumed a direct proportionality between force and tunnel current, which later experimental work[15] suggested may not hold for moderately doped semiconductor surfaces. Moreover, the calculations of Zotti et al.[14] suggested that the double lobe structure would be observed only within a specific range of (negative) bias voltages.

Most recently, an even more detailed theoretical study[16] convincingly showed that "double lobe" features with a similar spacing to that observed experimentally could be produced by tips modeled as dimer-terminated silicon clusters with adsorbed contaminants, providing an alternative explanation for the "double lobe" features. We note that multilobe features within the spatial size of a single atom in the *dissipation* channel have been reported during very close approach,[17] although these

Received: November 11, 2013
Revised: March 10, 2014
Published: March 14, 2014

   dx.doi.org/10.1021/nl4041803 | *Nano Lett.* 2014, 14, 2265−2270

clearly have a different origin to the "double lobe" features discussed above.

In parallel with the debate focused on the silicon−silicon system, further experimental results suggested that different symmetric structures could be observed using a graphite surface to probe a tungsten tip,[18] and in this instance the features were assigned to different crystallographic orientations of the tip apex. This work was followed up with a more detailed study where tungsten tips were imaged by single carbon monoxide molecules absorbed on a Cu(111) surface.[19] Again, "subatomic" features were observed and assigned to different multipole charges induced on the frontmost tungsten atom due to the different crystallographic orientations. A detailed theoretical study was performed shortly afterward, which suggested that the same features could be observed in simulation.[20] However, it was not possible to reach a definitive interpretation of the experimental results, as, depending on the tip orientation, the simulations suggested that subatomic resolution could occur either as a result of the induced charge density at the tip apex or due to the back bonding of the terminating atom.

It is at this juncture necessary to clarify the nomenclature to be used throughout the rest of the paper. It is trivial to show that features can be observed in both STM and AFM that have a spatial resolution smaller than the apparent size of a single atom. In STM, a particularly elegant example is the demonstration that information can be encoded with subatomic spatial resolution in the electronic density of states associated with the electron waves at the surface of a metal crystal.[21] However, although in this instance the features are subatomic in size, they are not assigned as having arisen from "inside" a single atom. In regard to DFM, our group recently demonstrated submolecular resolution on a tip-absorbed C_{60}, which produces what could be termed subatomic contrast on each adatom of the Si(111) surface[7] (with feature spacings similar to that reported in the original observation of subatomic features). But here it is unambiguous that the multiple features within the atoms originate not from any subatomic feature, but rather from the five atoms of a pentagon face of the C_{60}, compressed in size due to the relative flexibility of the tip. Consequently, we wish to make it clear that there is no controversy as to whether features with a smaller spatial size than a single atom can be observed in SPM. The controversy is only in regard as to whether these features truly arise from inside a single atom, i.e., whether they are truly subatomic in origin. From this point on, we will use the term "subatomic-like" to refer to features of the first kind (i.e., those features that have a spatial resolution smaller than a single atom but which arise as a result of multiatom interaction), and "true subatomic" to refer to features that arise from inside a single atom.

In this paper, we unambiguously show that subatomic-like features can arise from the back-bonding configuration of a surface atom being imaged during DFM. This is done by utilizing the change in bonding configuration of the surface adatoms of the Si(111) unit cell between the faulted and unfaulted half. Because of this change in symmetry across the unit cell, the features we observe cannot be assigned to any tip or feedback artifacts. At the same time, they suggest caution should be used when interpreting subatomic-like features, as our data cannot be interpreted as arising from within a single atom.

Experimental Methods. All experiments in this paper were carried out using an Omicron Nanotechnology LT STM/DFM in the qPlus configuration and carried out in a low-temperature cryostat cooled to approximately 78 K using liquid nitrogen in ultrahigh vacuum (UHV) (base pressure of 5×10^{-11} mbar or better). Clean Si(111) samples were prepared by the standard method of degassing a silicon wafer, flash heating to 1200 °C, quickly cooling to 900 °C and then slowly cooling to room temperature in order to obtain a good reconstruction. After preparation the silicon sample was transferred directly into the scan head for imaging. We used commercially supplied qPlus sensors from Omicron Nanotechnology, and these were introduced into the UHV chamber and then directly into the scan head without any further preparation.

When we first introduce the sensors and approach to the surface, we rarely obtain atomic resolution immediately, most likely due to the oxide layer that forms on electrochemically etched tungsten wires. Consequently, we prepare our tips by standard STM methods, including tip pulsing and controlled crashes into the surface. This is done until good STM resolution is obtained. We then usually select a small area and switch to DFM imaging.

Normally, after this form of tip preparation, we obtain "conventional" resolution of the silicon adatoms. This suggests that the tip has a strong chemical interaction with the surface,[3,4,22] and the adatoms image as circular protrusions in constant frequency shift imaging. However, we very rarely observe "contrast inversion" where the adatoms image as depressions in constant Δf feedback.[23] We note explicitly that we only refer to imaging at 0 V_{gap} or very close to 0 V_{gap}, and hence to a different phenomenon to that reported where contrast inversion occurs due to the so-called "phantom force"[15] induced by large tunnel currents or any effect due to electronic crosstalk.[24]

In addition to imaging, we also present quantitative force data. This was acquired by taking a $\Delta f(z)$ measurement on an adatom and then a cornerhole of the surface. The cornerhole (off) data is then subtracted from the adatom (on) data in order to produce a "short-range" $\Delta f(z)$. This on versus off method (as used by Lantz et al.[22] and Ternes et al.[25]) removes the nonsite-specific long-range forces and produces a $\Delta f(z)$ curve containing only contributions from the short-range forces. This short-range $\Delta f(z)$ was then inverted to force using the Sader−Jarvis algorithm.[26] We explicitly note that this method only produces absolute short-range forces if the off curve contains no site-specific force contributions. Although the cornerhole is generally considered large enough to fulfill this criterion in DFM experiments, the data in this paper are likely acquired at much closer approach than conventional (attractive imaging) DFM experiments. Consequently, statements about the size and magnitude of the site-specific force are strictly only relative measurements of the tip−sample force over the adatom versus the tip−sample force over the cornerhole. If there is any residual site-specific contribution over the cornerhole, we would expect the resultant forces to systematically underestimate the true force by a small amount.

Below, we present images taken in both constant Δf feedback and constant height mode. In constant height mode, an attractive interaction is imaged as a decrease in frequency shift, and as such appears as a dark depression in a map of frequency shift. This is the opposite to constant Δf feedback imaging, where an attractive interaction means that the tip will pull back from the surface in order to maintain a constant frequency shift, and as such will image as a bright protrusion. During constant height imaging, a custom-built atom tracking unit[27] was used in

dx.doi.org/10.1021/nl4041803 | Nano Lett. 2014, 14, 2265−2270

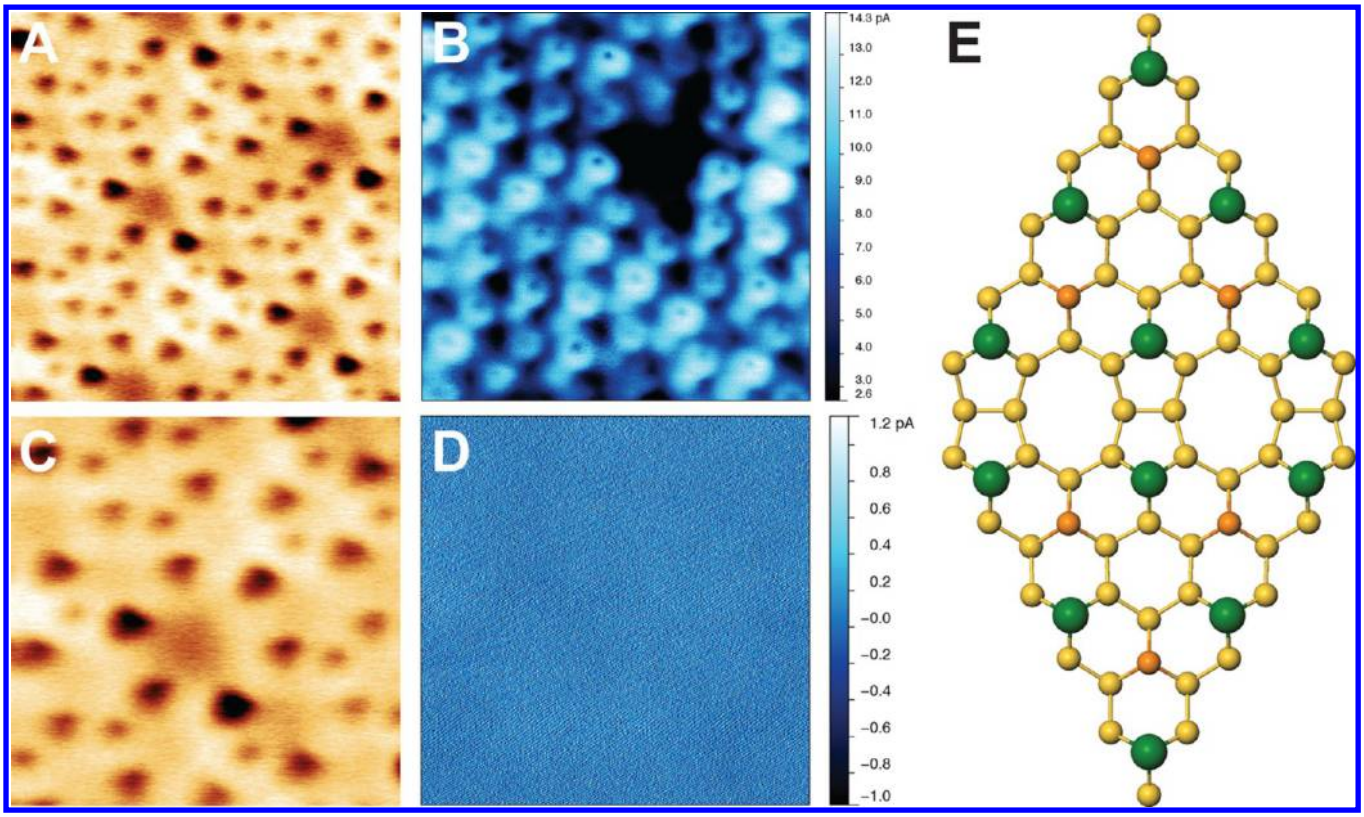

Figure 1. (A) Constant frequency shift image of the Si(111) 7 × 7 surface, showing inverted contrast and rest atom resolution, taken with Δf = −10.6 Hz, oscillation amplitude (A_0) = 275 pm, V_{gap} = +5 mV. (B) Simultaneously acquired tunnel current image. (C) High-resolution image of the same area taken with V_{gap} = 0 mV. (D) Simultaneously acquired tunnel current image. (E) Ball and stick model of the Si(111) 7 × 7 unit cell with adatoms highlighted in green and rest atoms highlighted in orange.

order to both measure, and then correct thermal drift by applying feedforward correction in between each scan.

Experimental Results. In Figure 1, we show results obtained shortly after approaching a clean, freshly prepared Si(111) sample with a newly introduced sensor. The measurements were conducted immediately after the first approach to the clean surface and consequently both tip and surface were as close as possible to their "native" state (i.e., clean silicon, tungsten oxide-coated tip).

After a short period of standard STM tip preparation, we obtained good STM resolution, and after switching to AFM we initially observed "conventional" resolution with a slight asymmetry on the adatoms.[28] However, during imaging we encountered a surface adsorbate, resulting in a slight tip change. After stopping and restarting the scan, we observed a striking change in contrast, shown in Figure 1A. The first feature of note is that the adatoms, and strikingly also the rest atoms, of the surface image as depressions rather than protrusions. The second feature is that the atoms have a very clear triangular symmetry, and that this symmetry changes between the faulted and unfaulted half of the unit cell. We also observe a different form of subatomic-like resolution in the simultaneously acquired tunnel current signal, with a decrease in the recorded tunnel current at the very center of the adatoms. However, we note that in this instance we cannot completely discount the effect on the recorded tunnel current due to the topographic feedback, and we do not necessarily assign an unambiguous physical interpretation to the tunnel current data. Importantly, the subatomic-like features in the topography remain present when the gap voltage was reduced to 0 V and no tunnel current was recorded (Figure 1C,D).

In order to simplify the interpretation of the imaging, we switched to imaging in constant height mode in the same region. Figure 2 shows a series of images taken at decreasing tip−sample distance, showing the progression in contrast as the tip approaches the surface. Far from the surface we observed no site-specific interaction (Figure 2A), but slightly closer we observed a very weak attractive interaction over the adatoms (Figure 2B). We note here that for "conventional" imaging the adatoms would continue to image as dark circles (i.e., attractive interaction) with increasing intensity for several angstroms. With this tip, however, we notice a completely different type of interaction: as stepping in we immediately see a switch to repulsive contrast (Figure 2C), which becomes more intense as the tip approaches the surface (Figure 2D,F). Importantly, we also observe the exact same triangular shape of the surface atoms, and the same switch in triangular symmetry across the two halves of the unit cell, as was observed in constant Δf feedback. At very close approach, we also observe an attractive feature in the center of the triangles (Figure 2F), which we will return to below.

By comparing the images shown in both Figures 1 and 2 with the ball and stick model of the Si(111) unit cell shown in Figure 1E, it is immediately clear that the only surface feature that shares the triangular symmetry of the adatoms is the back bonding configuration of those same atoms. Consequently, we are able to use the switch in the symmetry of the back bonding between the faulted and unfaulted half to unambiguously assign the triangular symmetry to the back-bonding configuration.

dx.doi.org/10.1021/nl4041803 | Nano Lett. 2014, 14, 2265−2270

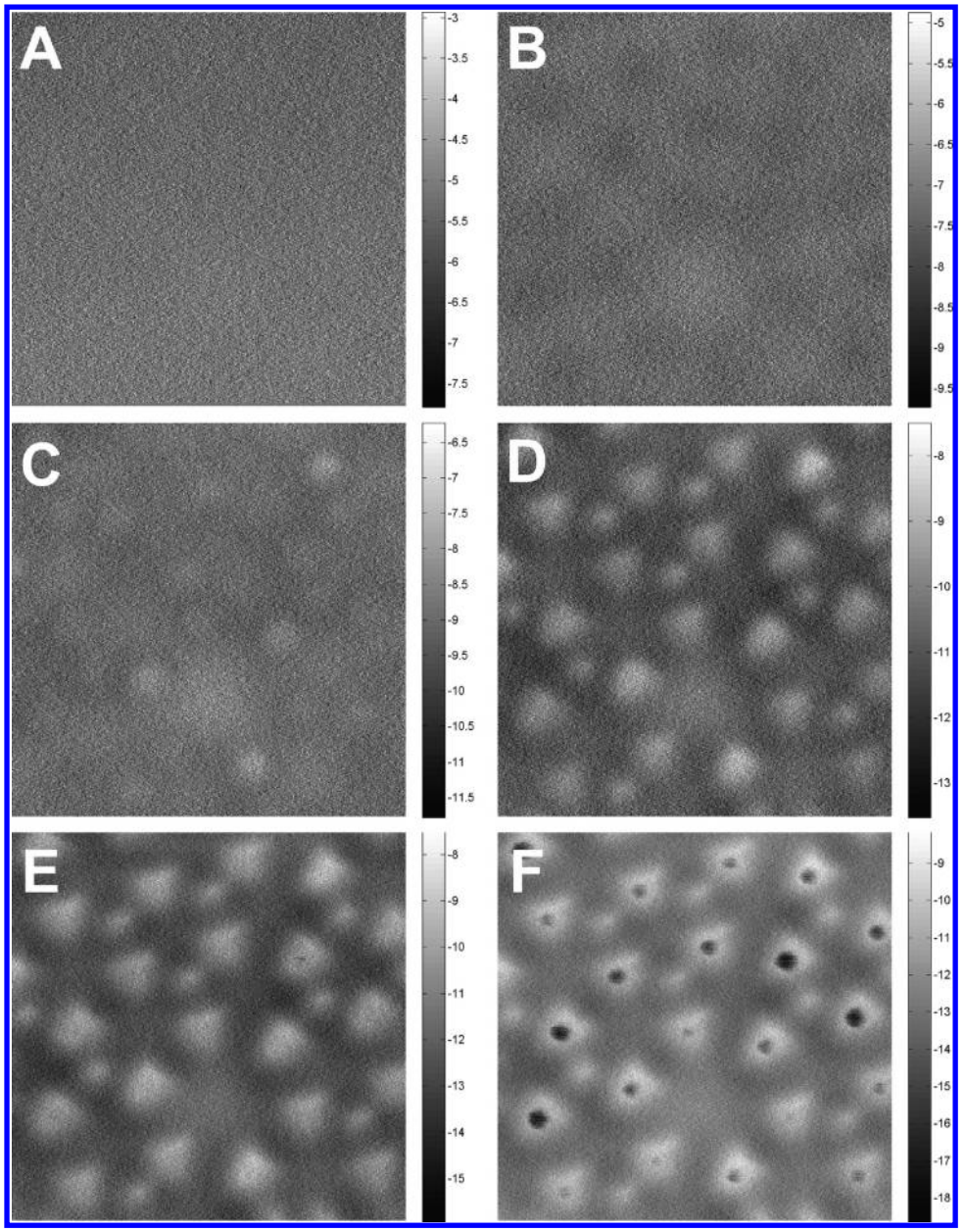

Figure 2. Sequence of constant height frequency shift images taken with decreasing tip sample height. Oscillation amplitude = 275 pm. *Z* heights are given relative to the atom tracking feedback position of −10.6 Hz. (A) Z = +300 pm, (B) Z = +157 pm, (C) Z = +90 pm, (D) Z = +36 pm, (E) Z = +30 pm, and (F) Z = −80 pm.

Were the triangular shape to arise from the tip, or any other aspect of the adatoms, then we would not expect to see any change between the faulted and unfaulted half (other than perhaps a change in intensity, rather than a change in symmetry).

At this juncture, some attention must be given to explaining the origin of the contrast we observe. Typically only the adatoms of the Si(111) surface are imaged during conventional AFM, and these are imaged as protrusions in constant frequency shift mode. Consequently, our tip must have radically different properties to those normally used.

We are able to obtain quantitative information about the tip−sample interaction by performing "force spectroscopy" experiments on the adatoms. Figure 3 shows the results of force spectroscopy measurements made on the adatoms as described in the Experimental Methods. The most important feature to note is the extremely small initial minimum in the attractive force between the tip and the atom on the order of 10−50 pN. This is almost two orders of magnitude smaller than typical interactions measured between a silicon cluster and a silicon surface (i.e., approximately 2 nN).[3,4,22] We assign this very small force as being the result of a passivated tip, similar to those described previously.[3,29,30] This very small attractive force helps to explain the contrast inversion observed in constant Δf feedback by taking into account the total Δf values measured. It must be remembered that in NC-AFM the frequency shift is determined not only by the short-range interaction (as discussed above) but also by the long-range van der Waals and electrostatic interaction. Consequently, by inspection of the Δf curves with respect to the $F(z)$ curve, it is clear that during constant Δf feedback at −10.6 Hz the tip had already entered the repulsive branch of the (site specific) force, and stable

dx.doi.org/10.1021/nl4041803 | *Nano Lett.* 2014, 14, 2265−2270

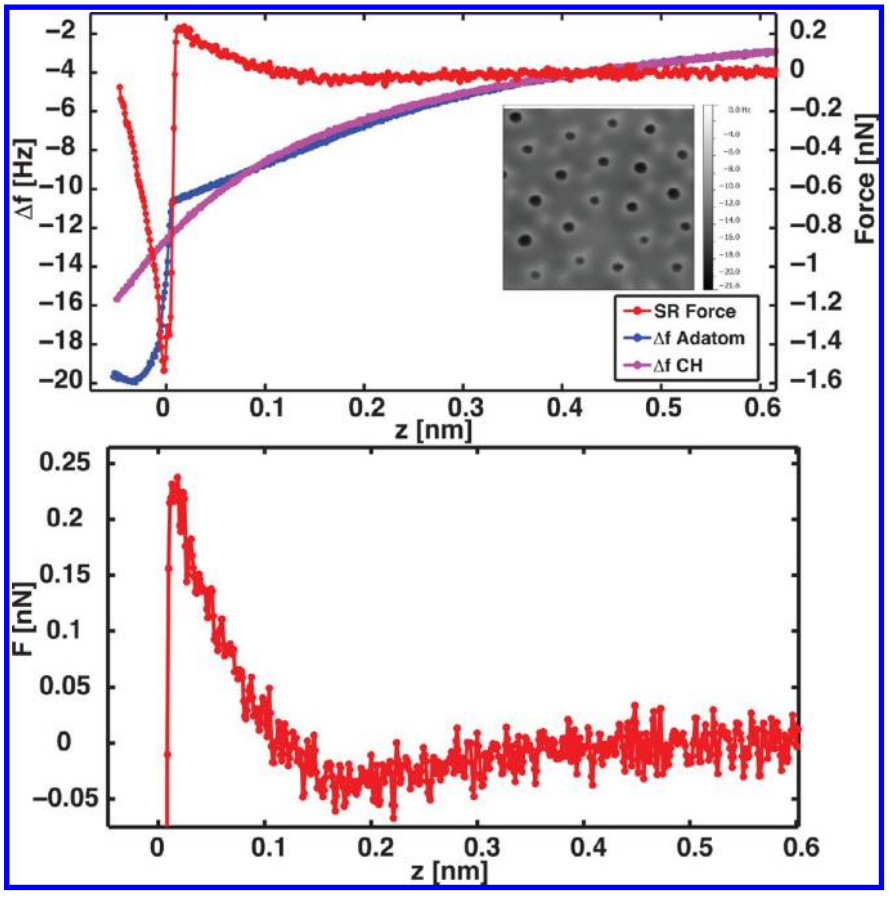

Figure 3. (A) Raw $\Delta f(z)$ curves acquired above an adatom and cornerhole in the image shown (inset). Also plotted is the site specific $F(z)$. $Z = 0$ corresponds to the imaging height. (B) Zoom of force curve showing the small attractive well and repulsive regime. From the overlay of the force and Δf, we can ascertain that during constant Δf imaging (Figure 1), feedback was occurring in the repulsive part of the short-range force, mediated by the long-range background.

feedback with negative frequency shifts was only mediated by the presence of the long-range background. This quantitative analysis of the force also explains the very weak attractive interaction we observed some distance from the surface during constant height imaging and therefore most likely arises from a highly suppressed chemical interaction, combined with local dispersion interactions.[31]

At close approach, we begin to see very strong repulsive behavior, which explains the repulsive contrast observed in Figure 2E. In addition, at very close approach we also observe a sudden jump in the force to large attractive values, which corresponds to the large depression feature observed in the center of the triangles. We suggest that this feature occurs due to a relaxation of the passivating element at the end of the tip, possibly exposing the reactive apex to the underlying surface adatom. We also note that similar (although clearly not identical) features were observed in DFT simulations that formed part of a combined experimental and theoretical study of different tip structures on a partly passivated Si(111) surface.[3]

Discussion. Because the symmetry of the surface in this instance allows us to unambiguously assign the subatomic-like contrast on the atoms to the back bonding, it is worth discussing the similarity of our data to other recent results showing subatomic contrast.

In Welker et al.[19] and Wright et al.,[20] when the foremost atom is back bonded with a 2-fold symmetry (W(110) tip) a 2-fold symmetry is present (both papers); when back bonded with a 3-fold symmetry (W(111) tip) a 3-fold symmetry is present (both papers); and back bonded with a 4-fold symmetry (W(100) tip) results in a circular symmetry experimentally[19] or circular/square symmetry in simulation.[20] In recent results from Hofmann et al.,[32] a circular symmetry was observed for both Cu(111) and Cu(100) tips, and a 2-fold symmetry for a Cu(110) tip. Consequently we note that an *n*-fold symmetry in the DFM data does not simply result from *n*-backbonding neighbors. Indeed, Wright et al. suggest that the charge density of the tip apex atom may be responsible for subatomic resolution in some cases, while in others it is the back bonding of the tip apex atom that produces the subatomic-like contrast. Intriguingly, their simulations suggest that it is the 3-fold structure that arises from the 3-fold symmetric backbonding of the tip, a feature with the same symmetry as the subatomic-like contrast in our data.

As noted above, we assign the contrast in our images to a passivated tip. Plausible candidates are tip-adsorbed H, OH, or CO, although we note that the same features were not observed with a partially (i.e., side-adsorbed) CO-terminated tip on Si(111) (Figure 3a of Welker et al.[31]). We also observe a marked increase in the occurrence of this contrast mode after deposition of molecules with passivated end groups,[33] and consequently it seems likely that the contrast arises from the passivation of the tip by an unreactive atom or molecule and the resulting suppression of the chemical interaction between the tip and surface.

dx.doi.org/10.1021/nl4041803 | *Nano Lett.* 2014, 14, 2265−2270

In the light of our results, it seems plausible that some cases of subatomic-like contrast do arise from variations in the tip−sample force due to the back-bonding configuration of the frontmost atom. It is not trivial to see how these effects can be distinguished from the angular bonding symmetry effects due to induced multipoles recently claimed to have been observed by Welker et al.,[19] especially if, as has been shown, subatomic-like features can also be observed in the attractive regime due to a flexible "multiapex" reactive tip.[7]

Conclusions. By the use of a passivated tip on the Si(111) 7 × 7 surface, we observe subatomic-like contrast on the adatoms. Because of the symmetry of the surface, we are able to unambiguously assign the subatomic-like contrast as arising from the back bonding of the adatoms to the surface and not to any feature "within" the atom itself, or due to any effect of the tip structure. These results suggest that more work is required in order to ascertain whether true subatomic resolution can be unambiguously observed and interpreted in DFM. In particular, careful thought must be given to the separation of back bonding and multitip effects in the interpretation of subatomic imaging experiments.

■ ASSOCIATED CONTENT

Supporting Information

Additional experimental results showing the tips state prior to the data presented in the main paper. This material is available free of charge via the Internet at http://pubs.acs.org.

■ AUTHOR INFORMATION

Corresponding Author

*E-mail: adam.sweetman@nottingham.ac.uk.

Notes

The authors declare no competing financial interest.

■ ACKNOWLEDGMENTS

P.M. and A.S. thank the Engineering and Physical Sciences Research Council (EPSRC) and the Leverhulme Trust, respectively, for Grants EP/G007837/1 and F00/114 BI. P.R. gratefully acknowledges financial support from the Alexander von Humboldt Foundation. The authors would like to acknowledge Samuel Paul Jarvis for numerous stimulating conversations and comments on the manuscript.

■ REFERENCES

(1) Binnig, G.; Rohrer, H.; Gerber, C.; Weibel, E. *Phys. Rev. Lett.* **1983**, *50*, 120−123.
(2) Sugimoto, Y.; Pou, P.; Custance, O.; Jelinek, P.; Abe, M.; Perez, R.; Morita, S. *Science* **2008**, *322*, 413−417.
(3) Yurtsever, A.; Sugimoto, Y.; Tanaka, H.; Abe, M.; Morita, S.; Ondráček, M.; Pou, P.; Pérez, R.; Jelínek, P. *Phys. Rev. B* **2013**, *87*, 155403.
(4) Sugimoto, Y.; Yurtsever, A.; Abe, M.; Morita, S.; Ondráček, M.; Pou, P.; Pérez, R.; Jelínek, P. *ACS Nano* **2013**, *7*, 7370−7376.
(5) Herz, M.; Giessibl, F.; Mannhart, J. *Phys. Rev. B* **2003**, *68*, 045301.
(6) Schull, G.; Frederiksen, T.; Arnau, A.; Sánchez-Portal, D.; Berndt, R. *Nature Chem.* **2010**, *6*, 23−27.
(7) Chiutu, C.; Sweetman, A. M.; Lakin, A. J.; Stannard, A.; Jarvis, S.; Kantorovich, L.; Dunn, J.; Moriarty, P. *Phys. Rev. Lett.* **2012**, *108*, 268302.
(8) Gross, L.; Mohn, F.; Moll, N.; Liljeroth, P.; Meyer, G. *Science* **2009**, *325*, 1110−1114.
(9) Giessibl, F. J.; Hembacher, S.; Bielefeldt, H.; Mannhart, J. *Science* **2000**, *289*, 422−425.
(10) Hug, H. J.; Lantz, M. A.; Abdurixit, A.; van Schendel, P. J. A.; Hoffmann, R.; Kappenberger, P.; Baratoff, A. *Science* **2001**, *291*, 2509a−2509.
(11) Giessibl, F. J.; Bielefeldt, H.; Hembacher, S.; Mannhart, J. *Ann. Phys. (Leipzig)* **2001**, *10*, 887−910.
(12) Huang, M.; Čuma, M.; Liu, F. *Phys. Rev. Lett.* **2003**, *90*, 256101.
(13) Caciuc, V.; Hölscher, H.; Blügel, S.; Fuchs, H. *Phys. Rev. Lett.* **2006**, *96*, 016101.
(14) Zotti, L. A.; Hofer, W. A.; Giessibl, F. J. *Chem. Phys. Lett.* **2006**, *420*, 177−182.
(15) Weymouth, A.; Wutscher, T.; Welker, J.; Hofmann, T.; Giessibl, F. *Phys. Rev. Lett.* **2011**, *106*, 226801.
(16) Campbellová, A.; Ondráček, M.; Pou, P.; Pérez, R.; Klapetek, P.; Jelínek, P. *Nanotechnology* **2011**, *22*, 295710.
(17) Sawada, D.; Sugimoto, Y.; Abe, M.; Morita, S. *Appl. Phys. Express* **2010**, *3*, 116602.
(18) Hembacher, S.; Giessibl, F. J.; Mannhart, J. *Science* **2004**, *305*, 380−383.
(19) Welker, J.; Giessibl, F. J. *Science* **2012**, *336*, 444−449.
(20) Wright, A. C.; Solares, S. D. *J. Phys. D: Appl. Phys.* **2013**, *46*, 155307.
(21) Moon, C. R.; Mattos, L. S.; Foster, B. K.; Zeltzer, G.; Manoharan, H. C. *Nat. Nanotechnol.* **2009**, *4*, 167−172.
(22) Lantz, M. A.; Hug, H. J.; Hoffmann, R.; van Schendel, P. J. A.; Kappenberger, P.; Martin, S.; Baratoff, A.; Güntherodt, H. J. *Science* **2001**, *291*, 2580−2583.
(23) Sweetman, A.; Jarvis, S.; Danza, R.; Moriarty, P. *Beilstein J. Nanotechnol.* **2011**, *3*, 25−32.
(24) Majzik, Z.; Setvín, M.; Bettac, A.; Feltz, A.; Cháb, V.; Jelínek, P. *Beilstein J. Nanotechnol.* **2012**, *3*, 249−259.
(25) Ternes, M.; González, C.; Lutz, C. P.; Hapala, P.; Giessibl, F. J.; Jelínek, P.; Heinrich, A. J. *Phys. Rev. Lett.* **2011**, *106*, 016802.
(26) Sader, J. E.; Jarvis, S. P. *Appl. Phys. Lett.* **2004**, *84*, 1801.
(27) Rahe, P.; Schütte, J.; Schniederberend, W.; Reichling, M.; Abe, M.; Sugimoto, Y.; Kühnle, A. *Rev. Sci. Instrum.* **2011**, *82*, 063704.
(28) Additional information can be found in the online Supporting Information.
(29) Sharp, P.; Jarvis, S.; Woolley, R.; Sweetman, A.; Kantorovich, L.; Pakes, C.; Moriarty, P. *Appl. Phys. Lett.* **2012**, *100*, 233120.
(30) Jarvis, S.; Sweetman, A.; Bamidele, J.; Kantorovich, L.; Moriarty, P. *Phys. Rev. B* **2012**, *85*, 235305.
(31) Welker, J.; Weymouth, A. J.; Giessibl, F. J. *ACS Nano* **2013**, *7*, 7377−7382.
(32) Hofmann, T.; Pielmeier, F.; Giessibl, F. J. *Phys. Rev. Lett.* **2014**, *112*, 066101.
(33) Sweetman, A.; Jarvis, S. P.; Rahe, P.; Champness, N. R.; Kantorovich, L.; Moriarty, P. Submitted.